Open Access Library Journal
2024, Volume 11, e11803
ISSN Online: 2333-9721
ISSN Print: 2333-9705

Spatial-Temporal Variation of Aerosol Optical Depth and Ångström Exponent over Selected Towns in Kenya: Environmental Impact and Climate Change

Stephen K. Mulago[1*], John W. Makokha[1], Richard Boiyo[2,3]

[1]Department of Science Technology and Engineering, Kibabii University, Bungoma, Kenya
[2]Department of Physical Sciences, Meru University of Science and Technology, Meru, Kenya
[3]Department of Environment, Water, Energy and Resources and Climate Change, County Government of Vihiga, Maragoli, Kenya
Email: *stevenkasuku8@gmail.com

How to cite this paper: Mulago, S.K., Makokha, J.W. and Boiyo, R. (2024) Spatial-Temporal Variation of Aerosol Optical Depth and Ångström Exponent over Selected Towns in Kenya: Environmental Impact and Climate Change. *Open Access Library Journal*, **11**: e11803.
https://doi.org/10.4236/oalib.1111803

Received: June 7, 2024
Accepted: July 26, 2024
Published: July 29, 2024

Abstract

Aerosol optical depth (AOD) and Ångström Exponent (AE) have become the most crucial metrics in assessing climate change. Despite this, studies related to AOD and AE are rare in Kenya. Using Moderate Resolution Imaging Spectroradiometer (MODIS) data, the present study analysed the spatial and temporal variations of aerosol optical depth at 550 nm (AOD_{550}) and examined the impact of these variations on AE over eight selected towns in Kenya during 2001-2021. The findings indicated high (0.22 ± 0.04) AOD during June-July-August-September (JJAS) and low (0.12 ± 0.04) values during March-April-May (MAM), all associated with prevailing local meteorological conditions. The Ångström Exponent in the wavelength (412 μm - 470 μm) was found to be high (1.1 - 1.7) in most towns, attributed to the dominance of fine-mode particles from increased anthropogenic activities. However, $AE_{412\text{-}470}$ exhibited relatively low values in the range of 0.7 to 1.0 in Garissa due to the dominance of coarse mode particles associated with increased dust particles. Also, the coastal regions of Kenya have moderate to high values of $AE_{412\text{-}470}$ associated with industrial emissions from the urbanized coastal regions of Mombasa. The study has contributed to an in-depth understanding of spatial-temporal variations of AOD and AE over the selected towns in Kenya and forms a scientific basis for further research on aerosol science over the region.

Subject Areas

Atmospheric Sciences

Keywords

MODIS, Aerosol Optical Depth, Ångström Exponent, Kenya

1. Introduction

Other than greenhouse gases and atmospheric ozone, atmospheric aerosols play a significant role in regional and global climate change [1]. They are emitted into the atmosphere or manufactured into the atmosphere through natural or anthropogenic means. Atmospheric aerosols are known to cause large uncertainties in climate change and the environment [2]. They affect climate through their interactions with solar and terrestrial radiations. Their climatic effects are divided into direct, indirect and semi-direct effects [3]. Atmospheric aerosols affect the climate through their interaction with solar and terrestrial thermal radiations [4]-[7]. Aerosols impact the Earth's climate directly by scattering and absorbing the incoming radiation from the Sun. Also, they affect climate indirectly by changing the microphysical properties of clouds. They change the size and density of cloud droplets thereby modifying the cloud albedo, cloud lifetime, cloud formation, and the probability of having precipitation [8] hence leading to cloud evolution [5] [9]. They also affect climate indirectly by serving as cloud condensation nuclei in liquid water clouds and ice nuclei in ice clouds [5]. In this case, each aerosol particle condenses one liquid cloud droplet, therefore, an increase in the number of aerosol particles increases the cloud condensation nuclei. Apart from their climatic effects, aerosols are known to affect human health and the environment [10]. They also affect visibility through the formation of haze in the atmosphere leading to poor vision by the transportation industry [11]. Notably, aerosols absorb solar radiation which in turn heats up the atmosphere. The heated atmosphere reduces the cloud fraction by evaporating water droplets and suppressing convection [9]. The absorption of solar radiation by aerosols modifies the vertical temperature profile thereby affecting cloud formation and other parameters such as the relative humidity and atmospheric stability. Because of the above uncertainties associated with the climatic effects of atmospheric aerosols, considerate efforts have been put in place to measure aerosols and cloud properties for adequate characterization at various spatial-temporal scales. Some of the commonly measured aerosol properties include the aerosol optical depth (AOD), Ångström exponent (AE) and absorption aerosol index (AAI). Meanwhile, Satellite-based remote sensors such as the Moderate Resolution Imaging Spectroradiometer (MODIS) in relation to the ground-based techniques data station, are rich in providing both spatial and long-term continuous observation of aerosol properties and therefore it is regarded to be the most appropriate for observing aerosol properties. Over a decade, a number of space-borne remote sensors such as Advanced Very High-Resolution Radiometer (AVHRR), Total Ozone Mapping Spectrometer

(TOMS), Moderate Resolution Imaging Spectroradiometer (MODIS), Multiangle Imaging Spectroradiometer (MISR), and Ozone Monitoring Instrument (OMI) [12]-[14] have generated a remarkable spatial and temporal characteristic of aerosols both regionally and globally. Furthermore, a number of studies have put concentrated efforts in assessing the spatiotemporal distributions and optical properties of aerosols and their research findings have been documented by several previous researchers [15]-[17]. Globally, Mehta *et al.* [18] reported increasing AOD trends in economically growing parts of Asia and decreasing trends over some parts of Europe, South America, and North America. Likewise, Using 13 years of Aqua-MODIS and OMI data over Kazakhstan, Boiyo *et al.* [19] reported an increasing trend in AOD over most areas of the country attributed to local meteorological conditions. Regionally, Using Terra satellite onboard the MODIS and MISR sensors, Adesina *et al.* [17] reported high AOD during summer due to the transportation of dust aerosols. Within East Africa, among a number of findings, Ngaina and Muthama [20] examined a high aerosol loading during the local dry period (December-February and June-August) using the MODIS data. Kumar *et al.* [21] Utilized AERONET Sun photometer aerosol products to investigate direct aerosol radiative forcing (DARF) and aerosol optical properties from 2011 to 2017 over an urban industrial city, Pretoria. They reported a decadal increase in the annual mean AOD and AE over different locations in South Africa, with high AOD during spring due to the presence of absorbing aerosols from biomass burning. Locally, Makokha *et al.* [22] over East Africa determined long-term annual and seasonal trends in total AOD at 550 nm and reported significant seasonality in AOD, with decreasing AOD trends over most regions of the study domain. Recently, Khamala *et al.* [23] over East Africa, reported an extensive distribution of AAOD 440 nm with high values noticed during the local dry seasons and low values over the wet seasons. In view of the immense increased aerosol concentration in Kenya which affects the local climate, very few studies have been conducted on aerosols and clouds and the relationship between aerosols and cloud properties. This knowledge is important for achieving a better understanding of aerosols in terms of trends and spatiotemporal distribution. This work, therefore, presents spatial and temporal variation of aerosol optical depth and Ångström Exponent. To understand the aerosol effects on climate, the Spatial and temporal variations of aerosol optical depth and Angstrom exponent have been obtained. The results derived from the present work give an extensive understanding of the spatial-temporal variations of aerosol optical depth and Ångström Exponent, which forms a scientific basis for further research on aerosol science over the region. The rest of this paper is structured as follows: Section 2 describes the study area and prevailing meteorological conditions, remotely sensed satellite data and methodology used in the present work, Section 3 presents results and discussions on spatial and temporal variation of aerosol optical depth and Ångström Exponent and lastly, Section 4 highlights the conclusion and recommendations obtained from the study.

2. Materials and Methods

2.1. Study Area

The Republic of Kenya, hereafter simply Kenya (Figure 1) has a geographical area of 582,646 km^2 stretching between 5˚S to 5˚N and 34˚E to 42˚E. It is neighbored by Uganda to the West, Somalia to the East, Ethiopia to the North, Tanzania to the South and Sudan to the North-west. Climatologically, the area is predominantly tropical with four seasons categorized according to rainfall patterns [24]. For instance, March-April-May and October-November-December are local wet seasons characterized by low AOD due to enhanced wet scavenging and reduced anthropogenic activities. On the contrary, the local dry seasons (January-February and June-July-August-September) are characterized by high AOD attributed to changes in meteorological conditions and emission sources [25]. The sources of aerosols in Kenya include biomass burning within and from neighboring agricultural zones, industrial and vehicular emissions especially for regions closer to major highways and urbanized areas [25] [26]. Additionally, sea salt from the Indian Ocean and aerosols from dust source regions (ASALs) form one of the major sources of natural aerosols in Kenya. [27] Other than the long-range transport of smoke particles from the DRC and Madagascar Island, Kenya also experiences sea salts from southwest parts of the Indian Ocean [28] [20] and dust aerosols from the Arabian Desert. In the present study, the aerosol parameters were analyzed over eight distinct geographical locations in Kenya which represent the cities of the provincial administration. They are Embu, Garissa, Kakamega, Kisumu, Mombasa, Nairobi, Nakuru and Nyeri.

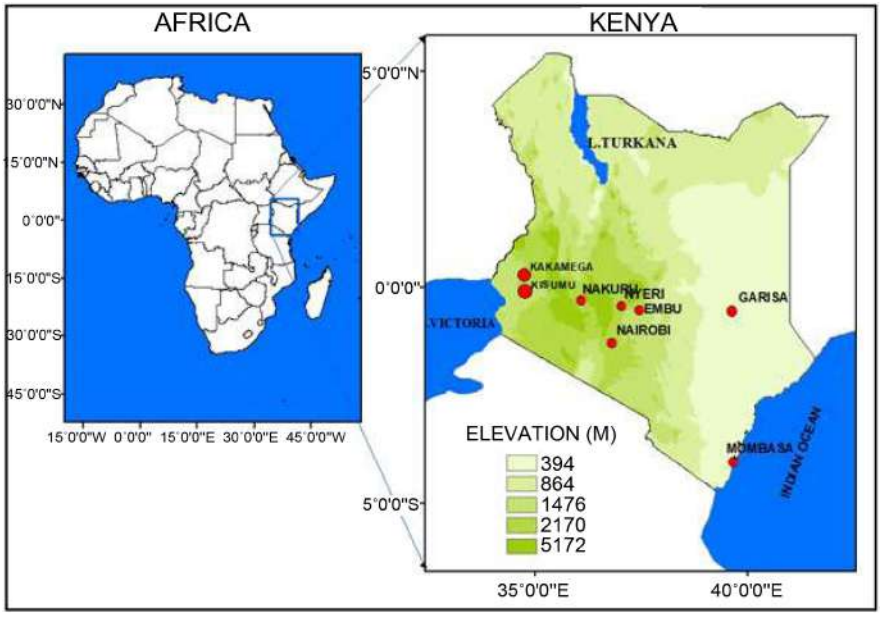

Figure 1. Map of the study area over the African continent (shown in the inset) with locations of eight sites used in this study marked with red dots shown on a topographic map. The areas shaded blue represent water bodies, while blue labelling shows major lakes in the study domain.

The regions have diverse climatic conditions and represent different aerosol regimes. A summary of the information regarding each of these selected towns is presented in Table 1.

Table 1. Geographical information about the eight study areas over Kenya.

	Latitude	Longitude	Altitude (m)	Prevailing climatic condition
Embu	0.66˚S	37.72˚E	1350	Urban region with vehicular emissions and solid waste deposits in river Githwariga.
Garissa	0.45˚S	39.65˚E	1138	Semi-arid regions dominated by desert dust aerosols.
Kakamega	0.28˚N	34.75˚E	1535	Rural/urban sites are dominated by agricultural and biomass burning.
Kisumu	0.09˚S	34.77˚E	1131	Urban/industrial region located on the borders of Lake Victoria.
Nairobi	1.34˚S	36.87˚E	1650	Urban/industrial area with significant anthropogenic activities.
Nakuru	0.43˚S	36.00˚E	1850	Evergreen region with agricultural activities.
Nyeri	0.42˚S	37.04˚E	1750	Rural region with agricultural activities and industrial emissions from the neighborhood.
Mombasa	3.98˚S	39.71˚E	50	A maritime region with a significant amount of sea salt deposits from the Indian Ocean.

2.2. Local Meteorology

The climate at the eight study sites is typical of Kenya, and by extension that of the entire East Africa [29] [30] except for the coastal regions, which are usually hot and humid, temperatures over the study domain are generally moderate, with maxima of around 25˚C and minima of 15˚C at an altitude of 1500 m [20]. The annual cycle of rainfall (Figure 2(a)) over the study domain exhibits a bi-modal distribution. The first season, which is the primary agricultural rain (due to its high reliability), is locally known as "the long rainfall" and occurs during March-April-May (MAM). The second season, locally known as "the short rainfalls" occurs in October-November-December (Figure 2(a)). The local "wet seasons" are generally characterized by reduced aerosol load due to large wet deposition of aerosols and high cloud effective radius as well as cloud fraction [2]. On the other hand, the local dry months, from June to September (JJAS) and January to February (JF), receive relatively shorter rainfall (Figure 2(a)) and are characterized by enhanced aerosol load and increased level of cloud fraction since the local dry seasons in Kenya were characterized by biomass burning and dust aerosols. The highest mean temperatures were recorded in February except

for Garissa which extended to march during the first local dry season and then decreased to a minimum value in June except for Garissa which attained its minimum value in July during the second local dry season (Figure 2(d)). The wind speed showed its maximum value (9 ms^{-1}) in July for Mombasa and Garissa and minimum (3 ms^{-1}) in June for Kisumu and Kakamega (Figure 2(b)). On the other hand, the relative humidity which affects the hygroscopic growth of aerosols, was high (80%) in July and November and low (30% - 40%) in February (Figure 2(c)).

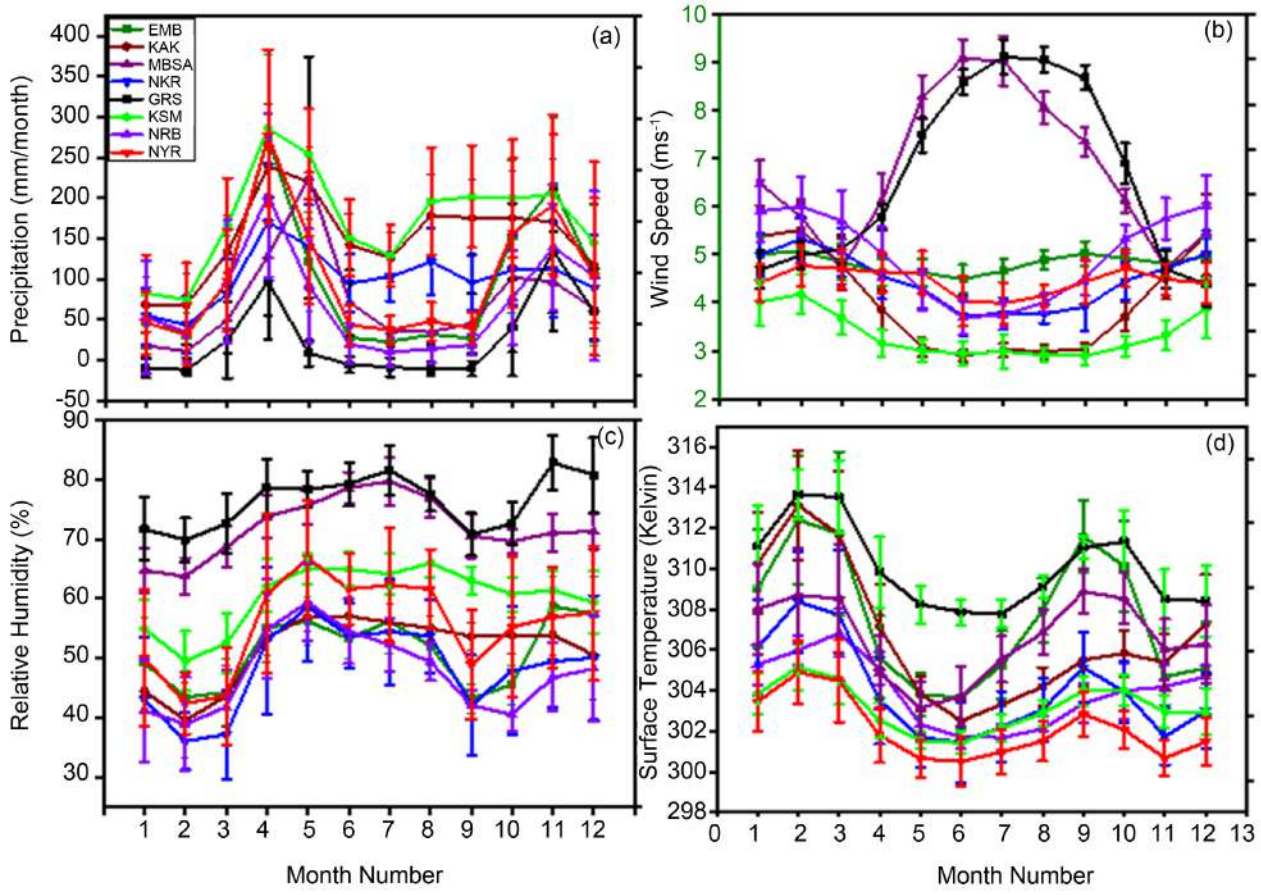

Figure 2. The time series variations of (a) Precipitation (mm/month), (b) Wind Speed (ms^{-1}), (c) Relative humidity (%), and (d) Surface Temperature (Kelvin) over selected towns in Kenya.

2.3. Remotely Sensed Satellite Data

Moderate Resolution Imaging Spectroradiometer (MODIS) is a satellite sensor that was brought into the earth's atmosphere by the National Aeronautics and Space Administration (NASA) in partnership with Goddard Space Flight Centre (GSFC). As a polar-orbiting sensor, it is divided into: MODIS Aqua which orbits at 13:30 p.m. local time in the afternoon and MODIS Terra orbiting at 10:30 a.m. local time in the morning. Using a temporal resolution of 1 - 2 days and a swath of 2330 km, MODIS obtains its data in 36 bands. Out of the 36 bands, 5 bands are at 500 m, 2 bands at 250 m and 29 bands at 1 km [31]-[33] with two algo-

rithms: Deep Blue (DB) and Dark Target (DT). The Deep Blue (DB) algorithm works best on brighter surfaces such as desert areas [30] [32], whereas the Dark Target (DT) on dark land [31]. The MODIS aerosol data are retrieved in different levels called collections. Recently, MODIS AOD product over land is operational on Collection 6.1 [34]. However, the Global validation exercises reported the weaknesses associated with retrieving AOD as ± (0.15 × AOD + 0.05) and (0.05 × AOD + 0.03) over the land and ocean respectively [31] [35]-[37]. Therefore, to reduce these errors, the MODIS aerosol data generation was bounded to pixels of surface reflectance more than 0.15 [38]. The present study used collection 6.1 (C6.1) Level 3 daily and monthly mean aerosol optical depth @550 nm, cloud effective radius, cloud top temperature, cloud top pressure, cloud water vapour and cloud fraction combined day and night, and Ångström exponent with spectral dependence between 412 and 470 micrometres over the land only. This spectral dependence for Ångström exponent was chosen since it is close to the top of the solar spectrum and therefore makes it more prone to the effects of solar radiation. The MODIS-Terra data products were retrieved from http://giovanni.gsfc.nasa.gov/ for a period of 20 years from January 2001 to December 2021. In addition to the MODIS-based remotely sensed data, the present study investigated the variation of the meteorological parameters including air temperature (˚C), relative humidity (%), wind speed (ms^{-1}) and rainfall (mm/day) which was observed over the selected towns from January 2001 to December 2021. The monthly averaged air temperature (˚C), relative humidity (%), wind speed (ms^{-1}) at 850 hPa and spatial resolution of 1˚ × 1˚ were obtained from Atmospheric Infrared Sounder (AIRS). Furthermore, the precipitation data at spatial resolutions of 0.25˚ × 0.25˚ was sourced from the Tropical Rainfall Measuring Mission (TRMM) preferably because of its better performance over the region [22] [39].

2.4. Methodology

2.4.1. Linear Regression Analysis

Linear regression analysis is used to predict the value of an unknown variable using the value of the known one. Notably, it estimates the relationship between dependable and independent variables. It also examines the relationship between them and predicts their future impact on each other in relation to climate change. For this purpose, the method has been discussed extensively by [40] and previously used by a number of studies such as [17] [41]-[43]. The method has the advantage of examining the magnitude and direction of trends in long-term data therefore preferred for this study. Linear regression uses the following derivation; by letting Y_t be the dependent variable whose value is to be predicted, and letting X_t be the independent variable representing time, "c" be the y-intercept which represents the value of Y_t at the beginning of the time series and ω be the slope or trend estimate of the dependent variable under consideration, and ε be the time series noise. Then the following equation is used to pre-

dict the dependent variable;

$$Y_t = c + \omega \times X_t + \varepsilon \tag{1}$$

The present work used this linear regression analysis to carry out the following tasks: 1) to investigate the relationship between aerosol optical depth and angstrom exponent and its impact on precipitation, 2) to ascertain the relationship between satellite-derived AOD at 550 nanometers and cloud parameters, and 3) to find the trend between aerosol optical depth and cloud parameters. The regression parameters such as the slope (ω) which represents the trend and y-intercept (c) serve as useful indicators of the temporal characteristics of aerosol optical depth (AOD) and angstrom exponent, and cloud parameters such as the cloud fraction, cloud optical depth, cloud effective radius and the cloud water vapour at a particular location and time. Therefore, the linear regression Equation (1) provides useful information concerning factors that affect the correlation.

2.4.2. Correlation Analysis

Correlation analysis is defined by a correlation coefficient (r) ranging from −1 to +1. When the value of r is +1 or −1, it indicates a perfect positive or negative correlation between given pairs of variables, respectively, with higher r suggesting better agreement. The correlation coefficients between two variables (e.g., X and Y) are calculated as follows;

$$\operatorname{corr}(X,Y) = \frac{\operatorname{cov}(X,Y)}{\sigma_x \cdot \sigma_y}. \tag{2}$$

where $\operatorname{cov}(X,Y)$ represents the covariance between X and Y, σ_x and σ_y are standard deviations of X and Y, respectively. In this work, correlation analysis was used to find the spatial characteristics of aerosol optical depth and angstrom exponent. Further, the spatial correlations of aerosol optical depth and Angstrom were computed using Level 3 annually averaged aerosol optical depth at 550 nm and Angstrom exponent with wavelength ranging from 412 to 470 micrometres. Therefore, the Correlation analysis formulae Equation (2) provides the level of the correlation in the spatial distribution of aerosol optical depth and Angstrom exponent.

3. Results and Discussion

3.1. Spatial and Temporal Variation of Aerosol Optical Depth and Angstrom Exponent

3.1.1. Annual Spatial Variation of Aerosol Optical Depth and Angstrom Exponent

The averaged spatial distribution of AOD_{550} and $AE_{412\text{-}470}$ over selected towns in Kenya observed during the study period (2001-2021) are illustrated in **Figure 3(a)** and **Figure 3(b)** respectively. The geophysical trends of annual mean AOD @550 nm obtained from MODIS Terra (combined Dark Target and Deep Blue) over Kenya are shown in **Figure 3(a)**. The spatial changes in the annual mean

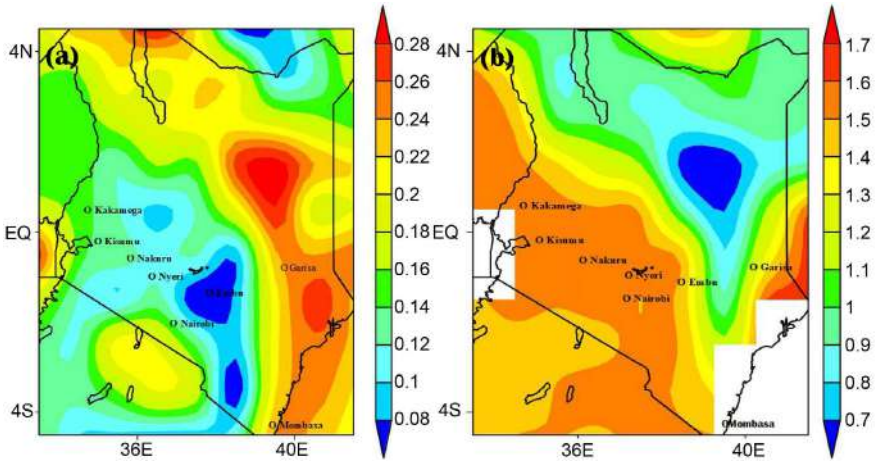

Figure 3. Annual mean spatial distribution of (a) AOD at 550 nm and (b) $AE_{412\text{-}470}$ over eight selected towns in Kenya for the period between 2001 and 2021.

AOD_{550} represents a general pattern of high, moderate, and low AOD, indicating distinct features of aerosol loading over different sites. On the contrary, the values of $AE_{412\text{-}470}$ were observed to vary between 0.7 and 1.7 with high values ($AE_{412\text{-}470}$ > 1) dominating in all the study regions (**Figure 3(b)**). Furthermore, High AOD values in the range 0.22 - 0.26, characterized by high values of $AE_{412\text{-}470}$ (>1) were found in Garissa. This is attributed to the transport of fine smoke particles by south easterly winds from the DRC, a region dominated by savannah and grassland fires. Furthermore, the anthropogenic activities prevalent in the region could release significant amounts of smoke particles and sulfate residues into the atmosphere leading to the enhanced AOD. Moderate AOD values (0.12 - 0.16) were found in Kakamega and Kisumu where high (>1) values of $AE_{412\text{-}470}$ were observed resulting from the difference in geographical conditions such as temperature, topography, humidity, etc., and differences in the source and transport of aerosols which are locally manufactured or imported from the neighboring towns into the regions. Also, the observed moderate AOD corresponding to high $AE_{412\text{-}470}$ could be associated with small amounts of smoke particles resulting from biomass burning and low levels of sulfates from sparse industries located around the region. Moreover, the Coastal regions of Kenya have moderate to high $AE_{412\text{-}470}$ values associated with industrial emissions from urbanized coastal regions of Mombasa [20] leading to enhanced AOD within the region. Also, the high AOD in Mombasa may result from Monsoon winds transporting aerosols to this region and the constant sea sprays from the Indian Ocean which serves as a sink to all atmospheric pollutants within the region. Low AOD_{550nm} (0.08 - 0.14) values characterized with high $AE_{412\text{-}470}$ were found in Nyeri, Nakuru and Nairobi attributed to anthropogenic activities which is characterized by low vegetation cover for Nyeri and Nakuru. Extremely very low AOD (0 - 0.08) characterized by high $AE_{412\text{-}470}$ values were noted in Embu attributed to small amounts of smoke particles resulting from biomass burning and low levels of sulfates from sparse industries located in the neighbuoring re-

gions. In addition to anthropogenic aerosols, geographical terrain in Embu as well as aerosol-climate interactions in the region play an important role in influencing aerosol loadings in the study domain.

3.1.2. Annual Temporal Variation of Aerosol Optical Depth and Angstrom Exponent

In terms of temporal variation, the mean AOD_{550} for the study period (2001-2021) is noticed to be highest over Garissa (0.23 ± 0.06) followed by Kisumu (0.15 ± 0.05), Kakamega (0.15 ± 0.04), Nairobi (0.13 ± 0.06), Embu (0.12 ± 0.04) and lowest in Nyeri (0.11 ± 0.04) and Nakuru (0.11 ± 0.04). The Seasonal variations of AOD_{550} (**Table 2**) depict maximum AOD during the JJAS (0.22 ± 0.04) followed by JF (0.13 ± 0.05), OND (0.13 ± 0.02) and low MAM (0.12 ± 0.04). In JF season, high AOD_{550} values in **Table 2** (> 0.22 ± 0.01) characterized with low AE (< 1) were noted in Garissa and Mombasa, moderate AOD_{550} (0.11 ± 0.00 to 0.13 ± 0.02) characterized high $AE_{412\text{-}470}$ (> 1) was noticed over Embu, Kakamega and Kisumu. On the other hand, low AOD_{550} values (0.06 ± 0.00 to 0.08 ± 0.00) corresponding to high $AE_{412\text{-}470}$ (> 1) were noticed over Nakuru and low $AE_{412\text{-}470}$ (< 1) over Nairobi and Nyeri respectively. This may be attributed to increased human activities such as land preparation and biomass burning in the regions (20) which could enhance the emission of smoke and dust particles into the atmosphere. Furthermore, the low AOD_{550} (**Table 2**) during MAM season was characterized by high $AE_{412\text{-}470}$ (> 1) over Embu, Kakamega, Kisumu and Nakuru (**Table 3**) and low $AE_{412\text{-}470}$ (< 1) over Garissa, Nairobi, Nyeri and Mombasa. This is more likely to result from the high aerosol deposition due to the long rains experienced during this season [20]. The same seasonal Changes were noted by [26] over Kenya. However, this implies that dust episodes were significantly reduced during the months of MAM in the study domain. Also, the small values of AOD_{550} observed in the season could be associated with low concentrations of aerosols like sulfates resulting from urban pollution preferably for the selected towns.

During JJAS, it is notable from **Table 2** that the eight selected towns have an enhanced average AOD_{550} characterized with high $AE_{412\text{-}470}$ ($AE_{412\text{-}470} > 1$) as seen in **Table 3** for Kisumu (1.58 ± 0.05), Embu (1.52 ± 0.02), Nakuru (1.52 ± 0.01), Kakamega (1.52 ± 0.00) and low $AE_{412\text{-}470}$ ($AE_{412\text{-}470} < 1$) for Garissa (0.67 ± 0.04), Nairobi (0.39 ± 0.01) and Nyeri (0.08 ± 0.01), associated with reduced rainfall [19]. It's also noted that the angstrom exponent has increased from the MAM season to JJAS season for most towns. As noted from the $AE_{412\text{-}470}$ values, there is a more considerable difference in aerosol size during the JJAS season. For instance, Nyeri is dominated by the coarse-mode aerosols from mineral dust originating from Arabian deserts and Indian Ocean sprays. With high $AE_{412\text{-}470}$ values, Kisumu, Embu, Nakuru and Kakamega may indicate fine-mode aerosols. The variability of $AE_{412\text{-}470}$ during the JJAS season as depicted in **Table 3** suggest that AE values over Garissa, Nairobi and Nyeri have a smaller variation while Kakamega has remained constant from MAM to JJAS season. Lastly, in the OND

season, high AOD_{550} (0.22 ± 0.03) in Table 2 characterized by extremely low $AE_{412\text{-}470}$ (−0.62 ± 0.55) in Table 3 was noticed over Mombasa, attributed to industrial emissions from urbanized coastal regions [20]. Furthermore, Moderate AOD_{550} values (0.10 ± 0.02 to 0.19 ± 0.06) characterized by high $AE_{412\text{-}470}$ (> 1) were reported in Embu, Kakamega and Kisumu and low $AE_{412\text{-}470}$ (< 1) in Garissa, were observed to be associated with dust aerosols locally produced [20] as well as transported from Saharan and Arabian Peninsula regions. However, low AOD_{550} (0.08 ± 0.01 to0.09 ± 0.01) characterized with high $AE_{412\text{-}470}$ (> 1) was noticed in Nakuru and low $AE_{412\text{-}470}$ (< 1) in Nyeri and Nakuru respectively. The variability in the AE over the eight selected towns signifies the variability in the aerosol size dominating the regions in the season.

Table 2. Temporal variation in AOD_{550} with standard (SD) deviation over selected towns in Kenya for the period between 2001 and 2021.

Month/ Season	EMBU AOD ± SD	GARISSA AOD ± SD	KAKAMEGA AOD ± SD	KISUMU AOD ± SD	NAIROBI AOD ± SD	NAKURU AOD ± SD	NYERI AOD ± SD	MOMBASA AOD ± SD
JAN	0.11 ± 0.03	0.21 ± 0.06	0.13 ± 0.07	0.15 ± 0.08	0.09 ± 0.05	0.09 ± 0.03	0.07 ± 0.03	0.28 ± 0.05
FEB	0.10 ± 0.03	0.23 ± 0.04	0.09 ± 0.05	0.10 ± 0.06	0.08 ± 0.04	0.06 ± 0.03	0.06 ± 0.03	0.25 ± 0.05
MAR	0.10 ± 0.03	0.22 ± 0.05	0.07 ± 0.03	0.08 ± 0.03	0.09 ± 0.04	0.06 ± 0.03	0.06 ± 0.03	0.21 ± 0.04
APR	0.10 ± 0.02	0.17 ± 0.07	0.08 ± 0.02	0.11 ± 0.03	0.13 ± 0.07	0.09 ± 0.04	0.09 ± 0.04	0.18 ± 0.03
MAY	0.11 ± 0.03	0.17 ± 0.07	0.14 ± 0.03	0.14 ± 0.03	0.16 ± 0.06	0.10 ± 0.03	0.10 ± 0.03	0.21 ± 0.04
JUN	0.20 ± 0.06	0.29 ± 0.08	0.27 ± 0.07	0.25 ± 0.07	0.25 ± 0.12	0.21 ± 0.07	0.21 ± 0.07	0.29 ± 0.04
JUL	0.21 ± 0.05	0.32 ± 0.08	0.29 ± 0.05	0.26 ± 0.05	0.24 ± 0.10	0.22 ± 0.06	0.22 ± 0.06	0.30 ± 0.04
AUG	0.14 ± 0.04	0.29 ± 0.05	0.21 ± 0.05	0.19 ± 0.06	0.16 ± 0.07	0.17 ± 0.05	0.17 ± 0.05	0.28 ± 0.04
SEP	0.10 ± 0.05	0.30 ± 0.07	0.15 ± 0.02	0.13 ± 0.04	0.09 ± 0.03	0.12 ± 0.04	0.12 ± 0.04	0.27 ± 0.04
OCT	0.07 ± 0.02	0.27 ± 0.04	0.12 ± 0.02	0.11 ± 0.03	0.07 ± 0.03	0.09 ± 0.03	0.09 ± 0.03	0.22 ± 0.03
NOV	0.11 ± 0.03	0.15 ± 0.07	0.12 ± 0.03	0.12 ± 0.04	0.08 ± 0.05	0.10 ± 0.04	0.10 ± 0.04	0.21 ± 0.03
DEC	0.12 ± 0.03	0.14 ± 0.06	0.12 ± 0.05	0.14 ± 0.08	0.09 ± 0.04	0.08 ± 0.03	0.08 ± 0.03	0.24 ± 0.05
Mean	0.12 ± 0.04	0.23 ± 0.06	0.15 ± 0.04	0.15 ± 0.05	0.13 ± 0.06	0.11 ± 0.04	0.11 ± 0.04	0.25 ± 0.04
JF	0.11 ± 0.00	0.22 ± 0.01	0.11 ± 0.02	0.13 ± 0.02	0.08 ± 0.00	0.06 ± 0.00	0.06 ± 0.00	0.27 ± 0.05
MAM	0.10 ± 0.00	0.19 ± 0.02	0.10 ± 0.03	0.11 ± 0.02	0.13 ± 0.03	0.08 ± 0.01	0.08 ± 0.01	0.20 ± 0.03
JJAS	0.16 ± 0.05	0.30 ± 0.01	0.23 ± 0.06	0.21 ± 0.05	0.19 ± 0.06	0.18 ± 0.04	0.18 ± 0.04	0.28 ± 0.04
OND	0.10 ± 0.02	0.19 ± 0.06	0.12 ± 0.00	0.13 ± 0.01	0.08 ± 0.01	0.09 ± 0.01	0.09 ± 0.01	0.22 ± 0.03

Table 3. Geographical information about the eight study areas over Kenya.

Month/ Season	EMBU AE ± SD	GARISSA AE ± SD	KAKAMEGA AE ± SD	KISUMU AE ± SD	NAIROBI AE ± SD	NAKURU AE ± SD	NYERI AE ± SD	MOMBASA AE ± SD
JAN	1.51 ± 0.01	0.9 ± 0.32	1.53 ± 0.03	1.52 ± 0.03	0.38 ± 0.53	1.50 ± 0.01	0.07 ± 0.03	−0.58 ± 0.89
FEB	1.50 ± 0.01	0.66 ± 0.23	1.52 ± 0.02	1.52 ± 0.02	0.34 ± 0.53	1.50 ± 0.00	0.06 ± 0.03	−0.21 ± 0.46
MAR	1.50 ± 0.01	0.80 ± 0.28	1.51 ± 0.01	1.51 ± 0.01	0.35 ± 0.53	1.50 ± 0.00	0.06 ± 0.03	−0.65 ± 0.57
APR	1.50 ± 0.02	0.93 ± 0.33	1.51 ± 0.01	1.51 ± 0.02	0.37 ± 0.54	1.51 ± 0.01	0.09 ± 0.04	−0.59 ± 0.54
MAY	1.51 ± 0.02	1.04 ± 0.34	1.52 ± 0.01	1.52 ± 0.02	0.38 ± 0.54	1.50 ± 0.00	0.10 ± 0.03	−0.96 ± 0.34

Continued

JUN	1.55 ± 0.04	0.69 ± 0.31	1.62 ± 0.05	1.62 ± 0.06	0.42 ± 0.53	1.53 ± 0.04	0.21 ± 0.07	−0.05 ± 0.99
JUL	1.52 ± 0.07	0.61 ± 0.29	1.64 ± 0.05	1.63 ± 0.06	0.41 ± 0.53	1.53 ± 0.06	0.22 ± 0.06	−0.56 ± 0.61
AUG	1.51 ± 0.03	0.72 ± 0.28	1.56 ± 0.04	1.54 ± 0.05	0.39 ± 0.52	1.52 ± 0.02	0.17 ± 0.05	−0.79 ± 0.68
SEP	1.50 ± 0.02	0.64 ± 0.28	1.53 ± 0.02	1.53 ± 0.02	0.36 ± 0.52	1.50 ± 0.01	0.12 ± 0.04	0.00 ± 0.00
OCT	1.51 ± 0.01	0.74 ± 0.19	1.52 ± 0.01	1.52 ± 0.02	0.34 ± 0.53	1.50 ± 0.01	0.09 ± 0.03	−0.79 ± 0.67
NOV	1.51 ± 0.02	1.07 ± 0.39	1.51 ± 0.01	1.52 ± 0.02	0.38 ± 0.54	1.50 ± 0.00	0.10 ± 0.04	0.00 ± 0.00
DEC	1.51 ± 0.02	0.99 ± 0.28	1.52 ± 0.01	1.51 ± 0.02	0.37 ± 0.54	1.51 ± 0.01	0.08 ± 0.03	−0.06 ± 0.98
Mean	1.51 ± 0.02	0.82 ± 0.29	1.54 ± 0.02	1.54 ± 0.03	0.37 ± 0.53	1.50 ± 0.04	0.11 ± 0.04	−0.35 ± 0.48
JF	1.51 ± 0.00	0.78 ± 0.12	1.54 ± 0.02	1.52 ± 0.00	0.36 ± 0.02	1.52 ± 0.01	0.06 ± 0.00	−0.39 ± 0.67
MAM	1.51 ± 0.00	0.92 ± 0.10	1.52 ± 0.00	1.51 ± 0.00	0.37 ± 0.01	1.50 ± 0.04	0.08 ± 0.01	−0.73 ± 0.15
JJAS	1.52 ± 0.02	0.67 ± 0.04	1.52 ± 0.00	1.58 ± 0.05	0.39 ± 0.02	1.52 ± 0.01	0.18 ± 0.04	−0.35 ± 0.57
OND	1.51 ± 0.00	0.93 ± 0.14	1.51 ± 0.01	1.52 ± 0.00	0.36 ± 0.02	1.50 ± 0.01	0.09 ± 0.01	−0.62 ± 0.55

4. Summary and Conclusions

This paper has provided a long-term (2001-2021) spatial and temporal variability of aerosol optical depth and Ångström Exponent over selected towns in Kenya and may form a basis for achieving a better and in-depth understanding of spatial and temporal variations in atmospheric aerosols over Kenya. The main conclusions drawn from the results are summarized as follows:

1) High AOD_{550} values characterized with high values of $AE_{412\text{-}470}$ were found in northeastern Kenya (Garissa), attributed to anthropogenic activities and transport of fine smoke particles by south easterly winds from the DRC, a region dominated by savannah and grassland fires leading to the enhanced AOD_{550}.

2) Moderate AOD550 characterized with high $AE_{412\text{-}470}$ was noticed in western Kenya (Kakamega) and Nyanza (Kisumu) could be associated with small amounts of smoke particles resulting from the biomass burning and low level of sulfates from sparse industries located around the region.

3) Low AOD_{550nm} values characterized with high $AE_{412\text{-}470}$ were found in (the central region of Kenya (Nyeri and Nairobi), and the rift valley of Kenya (Nakuru) attributed to anthropogenic activities which is characterized by low vegetation cover for Nyeri and Nakuru. Extremely very low AOD_{550} (0 - 0.08) characterized by high $AE_{412\text{-}470}$ values were noted in the eastern part of Kenya (Embu) attributed to small amounts of smoke particles resulting from the biomass burning and low level of sulfates from sparse industries located in the neighbuoring regions. In addition to anthropogenic aerosols, geographical terrain in Embu as well as aerosol-climate interactions in the region play an important role in influencing aerosol loadings in the study domain.

Acknowledgements

I express my sincere gratitude to individuals and institutions who contributed in various capacities to the work presented in this paper. Firstly, my deepest gratitude and respect goes to my supervisors Prof. John W. Makokha and Dr. Rich-

ard Boiyo for their constructive criticism that made the work successful. Thank you for agreeing to guide my master's research, for the inspirational ideas and for provoking my scientific novelty. I greatly admire your vast knowledge of everything, especially atmospheric aerosols, and I consider you excellent teachers and role models.

Secondly, I acknowledge the National Aeronautics and Space Administration (NASA) for setting up the framework, the Moderate Resolution Imaging Spectrometer (MODIS) and Tropical Rainfall Measuring Mission (TRMM) that furnished me with all kinds of data I required for this research to be a success. Additionally, I pass my sincere acknowledgment to the School of Graduate Studies and Department of Science, Technology and Engineering-Kibabii University for giving me an opportunity to further my education. You gave me an opportunity to get to know exciting people in the teaching and non-teaching fraternity. Thank you. To my colleagues, thank you for the moral and psychological support that you offered.

Lastly, I am always thankful to the Almighty God for the gift of life and strength He gave me during my studies. When things seemed not to work, He gave me hope in His word that He makes a way where there appears to be no way. This far is because of Him.

Conflicts of Interest

The authors have no conflict of interest whatsoever.

References

[1] Li, Z., Rosenfeld, D. and Fan, J. (2017) Aerosols and Their Impact on Radiation, Clouds, Precipitation, and Severe Weather Events. Oxford Research Encyclopaedia of Environmental Science. https://doi.org/10.1093/acrefore/9780199389414.013.126

[2] Nyasulu, M., Haque, M.M., Boiyo, R., Kumar, K.R. and Zhang, Y. (2020) Seasonal Climatology and Relationship between AOD and Cloud Properties Inferred from the MODIS over Malawi, Southeast Africa. *Atmospheric Pollution Research*, **11**, 1933-1952. https://doi.org/10.1016/j.apr.2020.07.023

[3] Rosenfeld, D., Sherwood, S., Wood, R. and Donner, L. (2014) Climate Effects of Aerosol-Cloud Interactions. *Science*, **343**, 379-380. https://doi.org/10.1126/science.1247490

[4] Twomey, S. (1977) The Influence of Pollution on the Shortwave Albedo of Clouds. *Journal of the Atmospheric Sciences*, **34**, 1149-1152. https://doi.org/10.1175/1520-0469(1977)034<1149:tiopot>2.0.co;2

[5] Charlson, R.J., Schwartz, S.E., Hales, J.M., Cess, R.D., Coakley, J.A., Hansen, J.E., *et al*. (1992) Climate Forcing by Anthropogenic Aerosols. *Science*, **255**, 423-430. https://doi.org/10.1126/science.255.5043.423

[6] Haywood, J. and Boucher, O. (2000) Estimates of the Direct and Indirect Radiative Forcing Due to Tropospheric Aerosols: A Review. *Reviews of Geophysics*, **38**, 513-543. https://doi.org/10.1029/1999rg000078

[7] Zhang, J. and Reid, J.S. (2010) A Decadal Regional and Global Trend Analysis of the Aerosol Optical Depth Using a Data-Assimilation Grade Over-Water MODIS and Level 2 MISR Aerosol Products. *Atmospheric Chemistry and Physics*, **10**, 10949-10963.

https://doi.org/10.5194/acp-10-10949-2010

[8] Rotstayn, L.D. and Lohmann, U. (2002) Tropical Rainfall Trends and the Indirect Aerosol Effect. *Journal of Climate*, **15**, 2103-2116. https://doi.org/10.1175/1520-0442(2002)015<2103:trtati>2.0.co;2

[9] Ramanathan, V., Crutzen, P.J., Kiehl, J.T. and Rosenfeld, D. (2001) Aerosols, Climate, and the Hydrological Cycle. *Science*, **294**, 2119-2124. https://doi.org/10.1126/science.1064034

[10] Boiyo, R., Kumar, K.R. and Zhao, T. (2017) Statistical Intercomparison and Validation of Multisensory Aerosol Optical Depth Retrievals over Three AERONET Sites in Kenya, East Africa. *Atmospheric Research*, **197**, 277-288. https://doi.org/10.1016/j.atmosres.2017.07.012

[11] Liao, W., Wang, X., Fan, Q., Zhou, S., Chang, M., Wang, Z., *et al*. (2015) Long-Term Atmospheric Visibility, Sunshine Duration and Precipitation Trends in South China. *Atmospheric Environment*, **107**, 204-216. https://doi.org/10.1016/j.atmosenv.2015.02.015

[12] Diner, D.J., Beckert, J.C., Reilly, T.H., Bruegge, C.J., Conel, J.E., Kahn, R.A., *et al*. (1998) Multi-Angle Imaging Spectroradiometer (MISR) Instrument Description and Experiment Overview. *IEEE Transactions on Geoscience and Remote Sensing*, **36**, 1072-1087. https://doi.org/10.1109/36.700992

[13] Tomasi, C., Fuzzi, S. and Kokhanovsky, A., Eds. (2017) Atmospheric Aerosols: Life Cycles and Effects on Air Quality and Climate. John Wiley & Sons.

[14] Torres, O., Bhartia, P.K., Herman, J.R., Ahmad, Z. and Gleason, J. (1998) Derivation of Aerosol Properties from Satellite Measurements of Backscattered Ultraviolet Radiation: Theoretical Basis. *Journal of Geophysical Research: Atmospheres*, **103**, 17099-17110. https://doi.org/10.1029/98jd00900

[15] Floutsi, A.A., Korras-Carraca, M.B., Matsoukas, C., Hatzianastassiou, N. and Biskos, G. (2016) Climatology and Trends of Aerosol Optical Depth over the Mediterranean Basin during the Last 12 Years (2002-2014) Based on Collection 006 MODIS-Aqua Data. *Science of the Total Environment*, **551**, 292-303. https://doi.org/10.1016/j.scitotenv.2016.01.192

[16] Kang, N., Kumar, K.R., Yin, Y., Diao, Y. and Yu, X. (2015) Correlation Analysis between AOD and Cloud Parameters to Study Their Relationship over China Using MODIS Data (2003-2013): Impact on Cloud Formation and Climate Change. *Aerosol and Air Quality Research*, **15**, 958-973. https://doi.org/10.4209/aaqr.2014.08.0168

[17] Adesina, A.J., Kumar, K.R., Sivakumar, V. and Piketh, S.J. (2016) Intercomparison and Assessment of Long-Term (2004-2013) Multiple Satellite Aerosol Products over Two Contrasting Sites in South Africa. *Journal of Atmospheric and Solar-Terrestrial Physics*, **148**, 82-95. https://doi.org/10.1016/j.jastp.2016.09.001

[18] Mehta, M., Singh, R., Singh, A., Singh, N. and Anshumali. (2016) Recent Global Aerosol Optical Depth Variations and Trends—A Comparative Study Using MODIS and MISR Level 3 Datasets. *Remote Sensing of Environment*, **181**, 137-150. https://doi.org/10.1016/j.rse.2016.04.004

[19] Boiyo, R., Kumar, K.R. and Zhao, T. (2018) Optical, Microphysical and Radiative Properties of Aerosols over a Tropical Rural Site in Kenya, East Africa: Source Identification, Modification and Aerosol Type Discrimination. *Atmospheric Environment*, **177**, 234-252. https://doi.org/10.1016/j.atmosenv.2018.01.018

[20] Ngaina, J., Mutai, B., Ininda, J. and Muthama, J. (2014) Monitoring Spatial-Temporal Variability of Aerosol over Kenya. *Ethiopian Journal of Environmental Studies and*

Management, **7**, 244-252. https://doi.org/10.4314/ejesm.v7i3.3

[21] Zhao, C., Yang, Y., Fan, H., Huang, J., Fu, Y., Zhang, X., Menenti, M., *et al*. (2020) Aerosol Characteristics and Impacts on Weather and Climate over the Tibetan Plateau. *National Science Review*, **7**, 492-495. https://doi.org/10.1093/nsr/nwz184

[22] Makokha, J.W., Odhiambo, J.O. and Godfrey, J.S. (2017) Trend Analysis of Aerosol Optical Depth and Ångström Exponent Anomaly over East Africa. *Atmospheric and Climate Sciences*, **7**, 588-603. https://doi.org/10.4236/acs.2017.74043

[23] Khamala, G.W., Makokha, J.W., Boiyo, R. and Kumar, K.R. (2023) Spatiotemporal Analysis of Absorbing Aerosols and Radiative Forcing over Environmentally Distinct Stations in East Africa during 2001-2018. *Science of the Total Environment*, **864**, Article ID: 161041. https://doi.org/10.1016/j.scitotenv.2022.161041

[24] Wang, Y., Xia, W., Liu, X., Xie, S., Lin, W., Tang, Q., Zhang, G.J., *et al*. (2021) Disproportionate Control on Aerosol Burden by Light Rain. *Nature Geoscience*, **14**, 72-76. https://doi.org/10.1038/s41561-020-00675-z

[25] Makokha, J.W. and Angeyo, H.K. (2013) Investigation of Radiative Characteristics of the Kenyan Atmosphere Due to Aerosols Using Sun Spectrophotometry Measurements and the COART Model. *Aerosol and Air Quality Research*, **13**, 201-208. https://doi.org/10.4209/aaqr.2012.06.0146

[26] Boiyo, R., Kumar, K.R. and Zhao, T. (2017) Statistical Intercomparison and Validation of Multisensory Aerosol Optical Depth Retrievals over Three AERONET Sites in Kenya, East Africa. *Atmospheric Research*, **197**, 277-288. https://doi.org/10.1016/j.atmosres.2017.07.012

[27] Makokha, S.N., Makokha, J.W. and Kelonye, F.B. (2022) Long-Term Assessment of the Spatial Temporal Trends in Selected Cloud Physical Properties over the Three Distinct Sites in Kenya. *Open Access Library Journal*, **9**, 1-18. https://doi.org/10.4236/oalib.1109582

[28] van der Werf, G.R., Randerson, J.T., Giglio, L., Collatz, G.J., Mu, M., Kasibhatla, P.S., *et al*. (2010) Global Fire Emissions and the Contribution of Deforestation, Savanna, Forest, Agricultural, and Peat Fires (1997-2009). *Atmospheric Chemistry and Physics*, **10**, 11707-11735. https://doi.org/10.5194/acp-10-11707-2010

[29] Ongoma, V. and Chen, H. (2016) Temporal and Spatial Variability of Temperature and Precipitation over East Africa from 1951 to 2010. *Meteorology and Atmospheric Physics*, **129**, 131-144. https://doi.org/10.1007/s00703-016-0462-0

[30] Ntwali, D., Ogwang, B.A. and Ongoma, V. (2016) The Impacts of Topography on Spatial and Temporal Rainfall Distribution over Rwanda Based on WRF Model. *Atmospheric and Climate Sciences*, **6**, 145-157. https://doi.org/10.4236/acs.2016.62013

[31] Levy, R.C., Remer, L.A. and Dubovik, O. (2007) Global Aerosol Optical Properties and Application to Moderate Resolution Imaging Spectroradiometer Aerosol Retrieval over Land. *Journal of Geophysical Research*: *Atmospheres*, **112**, D13210. https://doi.org/10.1029/2006jd007815

[32] Hsu, C.W., Chang, C.C. and Lin, C.J. (2003) A Practical Guide to Support Vector Classification. Technical Report, Department of Computer Science and Information Engineering, University of National Taiwan.

[33] Lam, T. and Hsu, C.H.C. (2006) Predicting Behavioral Intention of Choosing a Travel Destination. *Tourism Management*, **27**, 589-599. https://doi.org/10.1016/j.tourman.2005.02.003

[34] Levy, R.C., Remer, L.A., Kleidman, R.G., Mattoo, S., Ichoku, C., Kahn, R., *et al*. (2010) Global Evaluation of the Collection 5 MODIS Dark-Target Aerosol Products

over Land. *Atmospheric Chemistry and Physics*, **10**, 10399-10420. https://doi.org/10.5194/acp-10-10399-2010

[35] Kaufman, Y.J., Tanré, D., Remer, L.A., Vermote, E.F., Chu, A. and Holben, B.N. (1997) Operational Remote Sensing of Tropospheric Aerosol over Land from EOS Moderate Resolution Imaging Spectroradiometer. *Journal of Geophysical Research*: *Atmospheres*, **102**, 17051-17067. https://doi.org/10.1029/96jd03988

[36] Tanré, D., Kaufman, Y.J., Herman, M. and Mattoo, S. (1997) Remote Sensing of Aerosol Properties over Oceans Using the MODIS/EOS Spectral Radiances. *Journal of Geophysical Research*: *Atmospheres*, **102**, 16971-16988. https://doi.org/10.1029/96jd03437

[37] Remer, L.A., Kaufman, Y.J., Tanré, D., Mattoo, S., Chu, D.A., Martins, J.V., *et al*. (2005) The MODIS Aerosol Algorithm, Products, and Validation. *Journal of the Atmospheric Sciences*, **62**, 947-973. https://doi.org/10.1175/jas3385.1

[38] Acosta, D., Adelman, J., Affolder, T., Akimoto, T., Albrow, M.G., Ambrose, D., *et al*. (2005) Measurement of the J/ψ Meson and b-Hadron Production cross Sections in $p\bar{p}$ Collisions at s = 1960 GeV. *Physical Review D*, **71**, Article ID: 032001. https://doi.org/10.1103/physrevd.71.032001

[39] Kerandi, N.M., Laux, P., Arnault, J. and Kunstmann, H. (2016) Performance of the WRF Model to Simulate the Seasonal and Interannual Variability of Hydrometeorological Variables in East Africa: A Case Study for the Tana River Basin in Kenya. *Theoretical and Applied Climatology*, **130**, 401-418. https://doi.org/10.1007/s00704-016-1890-y

[40] Weatherhead, E.C., Reinsel, G.C., Tiao, G.C., Meng, X., Choi, D., Cheang, W., *et al*. (1998) Factors Affecting the Detection of Trends: Statistical Considerations and Applications to Environmental Data. *Journal of Geophysical Research*: *Atmospheres*, **103**, 17149-17161. https://doi.org/10.1029/98jd00995

[41] Kumar, K.R., Sivakumar, V., Yin, Y., Reddy, R.R., Kang, N., Diao, Y., *et al*. (2014) Long-Term (2003-2013) Climatological Trends and Variations in Aerosol Optical Parameters Retrieved from MODIS over Three Stations in South Africa. *Atmospheric Environment*, **95**, 400-408. https://doi.org/10.1016/j.atmosenv.2014.07.001

[42] Kumar, K.R., Yin, Y., Sivakumar, V., Kang, N., Yu, X., Diao, Y., *et al*. (2015) Aerosol Climatology and Discrimination of Aerosol Types Retrieved from MODIS, MISR and OMI over Durban (29.88˚S, 31.02˚E), South Africa. *Atmospheric Environment*, **117**, 9-18. https://doi.org/10.1016/j.atmosenv.2015.06.058

[43] Kang, N., Kumar, K.R., Hu, K., Yu, X. and Yin, Y. (2016) Long-term (2002-2014) Evolution and Trend in Collection 5.1 Level-2 Aerosol Products Derived from the MODIS and MISR Sensors over the Chinese Yangtze River Delta. *Atmospheric Research*, **181**, 29-43. https://doi.org/10.1016/j.atmosres.2016.06.008